

# Nitrosyl ruthenium complexes with general formula $[\text{RuCl}_3(\text{NO})(\text{P-P})]$ ( $\text{P-P} = \{\text{PPh}_2(\text{CH}_2)_n\text{PPh}_2\}$ , $n = 1-3$ and $\{\text{PPh}_2\text{-CH} = \text{CH-PPh}_2\}$ ). X-ray structure of $[\text{RuCl}_3(\text{NO})\{\text{PPh}_2(\text{CH}_2)_3\text{PPh}_2\}]$

Alzir A. Batista,<sup>a\*</sup> Cid Pereira,<sup>a</sup> Salette L. Queiroz,<sup>b</sup> Luiz A. A. de Oliveira,<sup>b</sup> Regina H. de A. Santos<sup>c</sup> and Maria Teresa do P. Gambardella<sup>c</sup>

<sup>a</sup> Departamento de Química/UFSCAR-CP, 676-CEP, 13565-905 São Carlos (SP), Brazil

<sup>b</sup> Instituto de Química/UNESP-CP, 355-CEP, 14800-900 Araraquara (SP), Brazil

<sup>c</sup> Instituto de Química de São Carlos/USP-CP, 780-CEP, 13560-970 São Carlos (SP), Brazil

(Received 15 May 1996; accepted 22 July 1996)

**Abstract**—Ruthenium(II) complexes with general formula  $[\text{RuCl}_3(\text{NO})(\text{P-P})]$  were obtained in the solid state, where  $\text{P-P} = \text{PPh}_2(\text{CH}_2)_n\text{PPh}_2$  ( $n = 1-3$ ) and  $\text{PPh}_2\text{-CH} = \text{CH-PPh}_2$ . The  $^{31}\text{P}$  NMR spectra of these compounds measured in  $\text{CH}_2\text{Cl}_2$  showed only singlets, consistent with a *fac* configuration containing two equivalent phosphorus atoms. However the X-ray diffraction data show that the  $[\text{RuCl}_3(\text{NO})\{\text{PPh}_2(\text{CH}_2)_3\text{PPh}_2\}]$  complex crystallizes in a *mer* configuration, where one of the phosphorus atoms is *trans* to the NO group, in a slightly distorted octahedral geometry. Copyright © 1996 Elsevier Science Ltd

**Keywords:** ruthenium; nitrosyl; complexes; biphosphines; X-ray structure; isomerism.

The nitrosyl ligand has been shown to exist in both linear and bent forms corresponding to three-electron and one-electron donors, respectively. Crystallographic and spectroscopic studies have been used to distinguish between these two geometries in mononuclear nitrosyl complexes [1–6]. There is some evidence that bulky ligands present in ruthenium nitrosyl complexes govern the intramolecular geometry of these species [7–9]. Thus, bulky ligands in the ruthenium complexes bend away from the nitrosyl group towards less sterically crowded sites in order to relieve the strain caused by these coordinating molecules. In the complex  $[\text{OsCl}_3(\text{NH}_3)(\text{PPh}_3)_2]$  [8], which contains an ammine ligand, less bulky than the

nitrosyl, the phosphines bend towards the  $\text{NH}_3$  by a small amount ( $0.3^\circ$ ) compared with  $[\text{RuCl}_3(\text{NO})(\text{P-Ph}_2\text{Me})]$ , where the phosphine bends away from the NO by a greater amount ( $4.1^\circ$ ) [9]. In this paper we report the preparation and characterization of ruthenium(II) complexes with general formula  $[\text{RuCl}_3(\text{NO})(\text{P-P})]$ , where P-P is one of the following diphosphine ligands: bis(diphenylphosphino)methane (dppm), 1,2-bis(diphenylphosphino)ethane (dppe), 1,3-bis(diphenylphosphino)propane (dppp), 1,2-bis(diphenylphosphino)ethylene (dppen), and the X-ray structure of the complex  $[\text{RuCl}_3(\text{NO})(\text{dppp})]$ . Our aim was mainly to provide information about the structure of this complex in solution and in the solid state, and to investigate the ability of coordinated  $\text{NO}^+$  to cause a *trans* strengthening effect in  $\{\text{Ru}^{\text{II}}-\text{NO}^+\}$ -type complexes containing strong  $\pi$  acceptor ligands.

\* Author to whom correspondence should be addressed.

## EXPERIMENTAL

## Measurements

The infrared spectra of the complexes were measured from powder samples diluted in CsI on an FT-IR Bomem-Michelson 102 spectrometer in the 4000–200  $\text{cm}^{-1}$  region. The  $^{31}\text{P}$   $\{^1\text{H}\}$  spectra were recorded in  $\text{CH}_2\text{Cl}_2$  on a Bruker 400 MHz spectrometer, with  $\text{H}_3\text{PO}_4$  (85%) as the internal reference.

## Synthesis

The  $[\text{RuCl}_3(\text{NO})\{\text{PPh}_2(\text{CH}_2)_n\text{PPh}_2\}]$  complexes were synthesized from  $[\text{RuCl}_3(\text{NO})]$ , which was prepared by passing a stream of NO through a solution of commercial ruthenium chloride (Degussa S.A.) in dichloromethane until the solution became red, followed by evaporation to dryness. The dried solid obtained was kept in a vacuum desiccator for at least 3 days before use. The NO was generated by reaction of dilute nitric acid (*ca* 33%) over copper metal. The NO gas was dried by passing it through a column containing anhydrous  $\text{CaCl}_2$ . A typical synthesis of the  $[\text{RuCl}_3(\text{NO})\{\text{PPh}_2(\text{CH}_2)_n\text{PPh}_2\}]$  complexes was done by refluxing for about 4 h the deoxygenated methanolic solution (5  $\text{cm}^3$ ) of  $[\text{RuCl}_3\text{NO}]$  (0.1 g, 0.42 mmol) and the corresponding diphosphine (0.42 mmol). In all cases solids were precipitated, which were filtered off and well washed with diethyl ether (yield: *ca* 80%).

$[\text{RuCl}_3(\text{NO})(\text{dppm})]$  (1). Orange microcrystalline powder. Found: C, 48.7; H, 3.4; N, 2.5. Calc. for  $\text{C}_{25}\text{H}_{22}\text{Cl}_3\text{NOP}_2\text{Ru}$ : C, 48.3; H, 3.6; N, 2.2%. IR:  $\nu(\text{NO})$  1867,  $\nu(\text{Ru}-\text{Cl})$  330 and 288  $\text{cm}^{-1}$ .  $^{31}\text{P}-\{^1\text{H}\}$  NMR:  $\delta$  -16.5.

$[\text{RuCl}_3(\text{NO})(\text{dppe})]$  (2). Yellow microcrystalline powder. Found: C, 49.3; H, 4.0; N, 2.1. Calc. for  $\text{C}_{26}\text{H}_{24}\text{Cl}_3\text{NOP}_2\text{Ru}$ : C, 49.1; H, 3.8; N, 2.2%. IR:  $\nu(\text{NO})$  1861,  $\nu(\text{Ru}-\text{Cl})$  331 and 278  $\text{cm}^{-1}$ .  $^{31}\text{P}-\{^1\text{H}\}$  NMR:  $\delta$  46.70.

$[\text{RuCl}_3(\text{NO})(\text{dppp})]$  (3). Yellow microcrystalline powder. Found: C, 49.4; H, 3.9; N, 2.2. Calc. for  $\text{C}_{27}\text{H}_{26}\text{Cl}_3\text{NOP}_2\text{Ru}$ : C, 49.9; H, 4.0; N, 2.2%. IR:  $\nu(\text{NO})$  1875,  $\nu(\text{Ru}-\text{Cl})$  325 and 291  $\text{cm}^{-1}$ .  $^{31}\text{P}-\{^1\text{H}\}$  NMR:  $\delta$  14.17.

$[\text{RuCl}_3(\text{NO})(\text{dppe})]$  (4). Yellow microcrystalline powder. Found: C, 49.7; H, 3.6; N, 2.2. Calc. for  $\text{C}_{26}\text{H}_{22}\text{Cl}_3\text{NOP}_2\text{Ru}$ : C, 49.3; H, 3.5; N, 2.2%. IR:  $\nu(\text{NO})$  1875,  $\nu(\text{Ru}-\text{Cl})$  330 and 283  $\text{cm}^{-1}$ .  $^{31}\text{P}-\{^1\text{H}\}$  NMR:  $\delta$  54.10.

## Crystal structure of 3

Suitable crystals of complex 3 were grown by slow evaporation of a dichloromethane/diethyl ether solution. A single crystal was used for data collection and cell parameter determination on an Enraf-Nonius CAD-4 diffractometer, with graphite-monochro-

ated Mo- $K_\alpha$  radiation at room temperature ( $T = 298$  K). Unit-cell parameters were obtained by least squares from the setting angles of 25 reflections. Intensity data were collected in the  $\omega$  scan mode up to  $\theta_{\text{max}} = 26.32^\circ$ , with scan rates between 3.3 and 16.5  $^\circ\text{min}^{-1}$ . The intensity of three standard reflections were essentially constant during the measurement. Data were corrected for Lorentz polarization and absorption effects using the empirical Psi Scan method [10]. The structure was solved using the SIR method [11] and difference Fourier techniques. In the final cycles of least-squares refinement, all non-hydrogen atoms were treated anisotropically. All hydrogen atoms were assumed in their calculated position by the geometry of the ligand atom and included in the least-squares calculation with a fixed isotropic temperature factor (6.0  $\text{\AA}^2$ ). The function minimized was  $\Sigma w(|F_o| - |F_c|)^2$ , where  $w^{-1} = \sigma^2(F_o)$ . Scattering factors for non-hydrogen atoms were taken from Cromer and Mann [12] with corrections for anomalous dispersion from Cromer and Liberman [13], and for hydrogen atoms from Stewart *et al.* [14].

All the calculations were performed with the system MoIEN [10]. The data collection and experimental details are summarized in Table 1. The relevant interatomic bond lengths and angles are listed in Table 2.

Table 1. Crystal data, data collection details and structure refinement results for  $[\text{RuCl}_3(\text{NO})\{\text{PPh}_2(\text{CH}_2)_3\text{PPh}_2\}]$

Molecular formula	$\text{C}_{27}\text{Cl}_3\text{H}_{26}\text{NOP}_2\text{Ru}$
Molecular weight	649.89
Crystal system	Monoclinic
Space group	$P2_1/c$
Z	4
$D_c$ ( $\text{g cm}^{-3}$ )	1.603
$a$ ( $\text{\AA}$ )	12.091(1)
$b$ ( $\text{\AA}$ )	13.973(1)
$c$ ( $\text{\AA}$ )	16.639(1)
$\beta$ ( $^\circ$ )	107.271(7)
$V$ ( $\text{\AA}^3$ )	2684.4(4)
$F(000)$	1312
Crystal size (mm)	$0.23 \times 0.25 \times 0.15$
$\lambda$ (Mo- $K_\alpha$ ) ( $\text{\AA}$ )	0.71073
$\mu$ ( $\text{cm}^{-1}$ )	10.1
Scan mode	$\omega-2\theta$
$\theta$ limits ( $^\circ$ )	2.33–26.32
Range of $hkl$ ; min.	0, -17, -20
Range of $hkl$ ; max.	15, 0, 20
Unique reflections	5447
Reflections used [ $I > 3\sigma(I)$ ]	3387
Number of variables	317
Goodness-of-fit	1.67
$R, R_w, R_{\text{all}}$	0.047, 0.056, 0.099
Max. shift/e.s.d.	0.01
Max., min. density in final difference map ( $\text{e \AA}^{-3}$ )	1.43, -0.18
Minimized function	$\Sigma w( F_o  -  F_c )^2$
Max., min. absorption correction (%)	99.99, 94.39

Table 2. Selected bond lengths (Å) and angles (°) for  $[\text{RuCl}_3(\text{NO})\{\text{PPh}_2(\text{CH}_2)_3\text{PPh}_2\}]$ , with esds in parentheses

Ru—Cl(1)	2.376(2)	P(1)—C(1b)	1.827(5)
Ru—Cl(2)	2.354(2)	P(1)—C(3)	1.832(6)
Ru—Cl(3)	2.366(2)	P(2)—C(1c)	1.833(6)
Ru—P(1)	2.460(1)	P(2)—C(1d)	1.813(6)
Ru—P(2)	2.436(2)	P(2)—C(1)	1.808(6)
Ru—N	1.880(4)	O—N	0.906(7)
P(1)—C(1a)	1.826(5)		
Cl(1)—Ru—Cl(2)	92.54(6)	Ru—P(1)—C(1a)	120.3(2)
Cl(1)—Ru—Cl(3)	176.64(5)	Ru—P(1)—C(1b)	113.1(2)
Cl(1)—Ru—P(1)	81.42(5)	Ru—P(1)—C(3)	107.8(2)
Cl(1)—Ru—P(2)	98.32(6)	C(1a)—P(1)—C(1b)	101.4(2)
Cl(1)—Ru—N	88.4(2)	C(1a)—P(1)—C(3)	107.5(3)
Cl(2)—Ru—Cl(3)	86.65(6)	C(1b)—P(1)—C(3)	105.7(3)
Cl(2)—Ru—P(1)	86.41(5)	Ru—P(2)—C(1c)	109.8(2)
Cl(2)—Ru—P(2)	167.31(6)	Ru—P(2)—C(1d)	125.0(2)
Cl(2)—Ru—N	93.0(2)	Ru—P(2)—C(1)	107.5(2)
Cl(3)—Ru—P(1)	95.27(5)	C(1c)—P(2)—C(1d)	99.8(2)
Cl(3)—Ru—P(2)	82.13(5)	C(1c)—P(2)—C(1)	108.1(3)
Cl(3)—Ru—N	94.9(2)	C(1d)—P(2)—C(1)	105.6(3)
P(1)—Ru—P(2)	88.72(5)	Ru—N—O	172.0(6)
P(1)—Ru—N	169.8(2)	P(2)—C(1)—C2	115.3(4)
P(2)—Ru—N	93.8(2)	P(1)—C(3)—C2	115.3(4)

Figure 1 shows the ORTEP [15] drawing of the molecule with the atom-numbering scheme.

## RESULTS AND DISCUSSION

In all the diphosphine complexes studied in this work, the  $\nu(\text{NO})$  in the infrared spectra were close to  $1870\text{ cm}^{-1}$ , indicating that they were indeed of the  $\{\text{Ru}^{\text{II}}-\text{NO}^+\}$  type [1,2].

The  $^3\text{P}\{-^1\text{H}\}$  NMR data mentioned in the experimental section show that these complexes present only a singlet, suggesting that in all cases the phosphorus atoms are *trans* to the chlorines. However, the crystal structure of the  $[\text{RuCl}_3(\text{NO})(\text{dppp})]$  complex (Fig. 1) shows that the NO group is *trans* to a phos-

phorus atom, suggesting that this compound can be found as a *fac* isomer in solution and prefers, probably because of steric effects, to be crystallized as a *mer* isomer.

The  $\nu(\text{NO})$  in the IR spectrum obtained from crystals of the  $[\text{RuCl}_3(\text{NO})(\text{dppp})]$  complex is at  $1841\text{ cm}^{-1}$ , different from the  $1875\text{ cm}^{-1}$  found for the sample prepared from powder of the same complex. Considering that the chlorine is a better donor than the phosphorus atom, in this case the back-bonding  $\text{Ru} \rightarrow \text{NO}$  should be more intense for the structure where the NO is *trans* to the chlorine (*fac* isomer) and the  $\nu(\text{NO})$  should be expected to shift to a lower energy, which was not observed experimentally. In this case the shift of  $34\text{ cm}^{-1}$  observed in the IR spectra

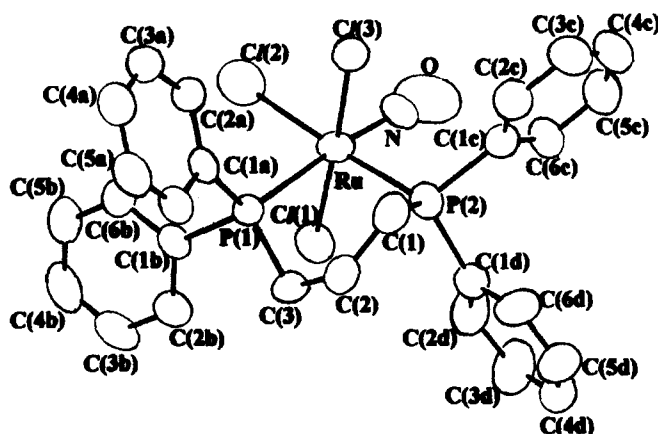


Fig. 1. Molecular structure and crystallographic numbering scheme for  $[\text{RuCl}_3(\text{NO})\{\text{PPh}_2(\text{CH}_2)_3\text{PPh}_2\}]$ .

of the samples probably is not due to electronic effects, but is the consequence of steric effects. Thus, when the nitrosyl group is close to three chlorine atoms (*mer* isomer) for steric reasons it becomes less linear, compared with the NO species which is only close to two chlorine atoms (*fac* isomer), and in this case the  $\nu(\text{NO})$  shifts to a lower energy [7]. For the crystal sample the IR spectra shows  $\nu_{\text{Ru-Cl}}$  at 336 and 311  $\text{cm}^{-1}$ .

It is interesting to point out that the isomerization process from the *mer* to the *fac* isomer was observed through  $^{31}\text{P}\{-^1\text{H}\}$  experiments. In this case the  $^{31}\text{P}\{-^1\text{H}\}$  spectra (A) of a fresh solution prepared with crystals of the  $[\text{RuCl}_3(\text{NO})(\text{dppp})]$  in  $\text{CH}_2\text{Cl}_2$  shows two doublets ( $\delta = 10.13$  and  $\delta = 0.27$ ,  $J_{\text{P-P}} = 48.6$  Hz) as expected for the *mer* isomer. The intensity of these two doublets decreased with time and the singlet at  $\delta = 14.17$ , which belongs to the *fac* isomer, appeared (B) and at the end of this isomerization process only this isomer was present in the solution (C) (Fig. 2).

In the structure of the  $[\text{RuCl}_3(\text{NO})(\text{dppp})]$  *mer* isomer (Fig. 1), three mutually perpendicular coordination planes are well defined and their angles are of a slightly distorted octahedron. Their angles are close to  $90^\circ$ . In this complex the Ru atom is displaced 0.099 Å towards the NO group, out of the best plane consisting of the three chlorines and the P(2) phosphorus atom. For the analogous series of *mer*- $[\text{RuX}_3(\text{NO})(\text{en})]$  complexes, where X = Cl, Br, I, these values were found to be 0.176(2), 0.1518(7) and 0.106(2) Å, respectively [16]. These distortions were attributed to the steric hindrance between the bulky Ru—NO bond orbital and the halogen. The distortion is decreased in the order Cl, Br, I because the bigger the halogen is the longer is the Ru—X length [average Ru—X lengths are 2.36, 2.50, 2.71 Å for X = Cl, Br and I, respectively]. This rationalization seems to be reasonable in order to explain the smaller value of the

distortion (0.099 Å) found for the  $[\text{RuCl}_3(\text{NO})(\text{dppp})]$  complex compared with those found for the halogen complexes  $[\text{RuX}_3(\text{NO})(\text{en})]$ , considering that the diphosphine is bulkier than the en ligand. This effect becomes evident when the average Ru—Cl distance in  $[\text{RuCl}_3(\text{NO})(\text{en})]$  and  $[\text{RuCl}_3(\text{NO})(\text{dppp})]$  are found to be essentially the same (*ca* 2.37 Å), but the Ru—N(2) and Ru—P(2), 2.092(9) [16] and 2.436(2) Å, respectively, are substantially different. In the case of  $[\text{RuCl}_3(\text{NO})(\text{dppp})]$  the average interatomic distance between the nitrogen atom of the NO and the chlorine ligands is 3.07 Å, identical to that found in the *mer*- $[\text{RuCl}_3(\text{NO})(\text{en})]$  complex [16]. The identical distances found in these two complexes can be rationalized if we consider that, although the diphosphine ligand is bulkier than the en ligand, this effect is compensated for by the longer Ru—P(2) distance.

The observed Ru—N—O bond angle [ $172.0(6)^\circ$ ] is smaller than those found for  $[\text{RuX}_3(\text{NO})(\text{en})]$  [16] [ $174.1(7)$ ,  $176.9(5)$  and  $179.4(2)^\circ$  for X = Cl, Br and I, respectively]. This effect is attributed to the repulsion between the extensive molecular orbital of the NO ligand and the phenyl rings bonded to the P(2) atom of the diphosphine. The same effect is reflected in the angle P(1)—Ru—N, which is smaller than  $180^\circ$  [ $169.8(2)^\circ$ ], and in the angles Cl(3)—Ru—P(2) [ $82.13(5)^\circ$ ] and Cl(1)—Ru—P(2) [ $98.32(6)^\circ$ ]. The bulky NO molecular orbitals show influence even in the Cl(2)—Ru—P(1) and the Cl(2)—Ru—N angles. As can be seen in Table 2 these angles are equal to  $86.41(5)$  and  $93.0(2)^\circ$ , respectively, which can be explained by considering that the NO molecular orbital pushes Cl(2) towards the P(1) atom. The Ru—P(1) and Ru—P(2) distances of 2.460(1) and 2.436(2) Å, respectively (see Table 2) are near to the expected values, which usually fall in the range 2.41–2.44 Å [17], and in this case the *trans* strengthening effect in the  $[\text{RuCl}_3(\text{NO})(\text{dppp})]$  complex was not observed. It is likely that the essentially linear nitrosyl group does not achieve strong bonding (particularly through Ru—NO  $\pi$  back-bonding) when *trans* to phosphorus, which is not a very good donor atom [18]. Indeed, this crystal structure shows the oxygen atom of the NO group with a high thermal parameter, indicating some flexibility for the orientation of the nitrosyl with respect to the Ru—N bond. The distance Ru—N is longer [1.880(4) Å] when NO is *trans* to the phosphine, as in our complex, than when it is *trans* to bromine [1.787(9) Å] or *trans* to oxygen from the ethylsulfoxide [1.72(1) Å] as in  $[\text{RuBr}_3(\text{NO})(\text{Pr}_2\text{S})_2]$  and  $[\text{RuBr}_3(\text{NO})(\text{Et}_2\text{S})(\text{Et}_2\text{SO})]$  complexes, respectively [19]. The Ru—N distance of 1.880(4) Å is a little larger than the expected metal—nitrogen double bond distance of 1.75(3) Å in ruthenium and osmium complexes that contain linear nitrosyl ligands [7]. The N—O distance [0.906(7) Å] is close to those found for the bis(dipropyl)sulfide [1.047(26) Å] and for the sulfide/sulfoxide [1.09(1) Å] complexes mentioned above [19].

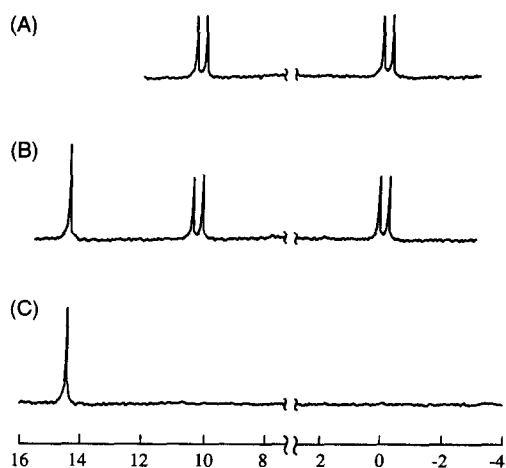


Fig. 2. (A)  $^{31}\text{P}\{-^1\text{H}\}$  NMR spectrum of a fresh solution at room temperature of  $[\text{RuCl}_3(\text{NO})\{\text{PPh}_2(\text{CH}_2)_3\text{PPh}_2\}]$  (*mer* isomer) in  $\text{CH}_2\text{Cl}_2$ . (B)  $^{31}\text{P}\{-^1\text{H}\}$  NMR spectrum of (A) after 3 h. (C)  $^{31}\text{P}\{-^1\text{H}\}$  NMR spectrum of (A) after 12 h.

*Supplementary material*—Atomic coordinates, anisotropic thermal parameters and a complete list of the bond distances and angles have been deposited with the Cambridge Crystallographic Data Centre.

*Acknowledgements*—This work was supported by grants from the FAPESP, CNPq, CAPES and FINEP.

#### REFERENCES

1. Bottomley, F., *Coord. Chem. Rev.*, 1978, **26**, 7.
2. Enemark, J. H. and Feltham, R. D., *Coord. Chem. Rev.*, 1974, **13**, 339.
3. Pierpont, C. G. and Eisenberg, R., *Inorg. Chem.*, 1972, **11**, 1088.
4. Gaughan, A. P. Jr, Corden, B. J., Eisenberg, R. and Ibers, J. A., *Inorg. Chem.*, 1974, **13**, 786.
5. Pierpoint, C. G. and Eisenberg, R., *Inorg. Chem.*, 1973, **12**, 199.
6. Seddon, E. A. and Seddon, K. R., *The Chemistry of Ruthenium*. Elsevier, Amsterdam, 1984, pp. 1130–1138.
7. Haymore, B. L. and Ibers, J. A., *Inorg. Chem.*, 1975, **14**, 3060.
8. Bright, D. and Ibers, J. A., *Inorg. Chem.*, 1969, **8**, 1078.
9. Schultz, A. J., Henry, R. L., Reed, J. and Eisenberg, R., *Inorg. Chem.*, 1974, **13**, 732.
10. Fair, C. K., *MoLEN: Structure Determination System*. Enraf–Nonius, Delft, The Netherlands, 1990.
11. Burla, M. C., Camalli, M., Cascarano, G., Ciacovazzo, C., Polidori, G., Spagna, R. and Viterbo, D., *J. Appl. Cryst.*, 1989, **22**, 389.
12. Cromer, D. T. and Mann, J. B., *Acta Cryst.*, 1968, **A24**, 321.
13. Cromer, D. T. and Liberman, D., *J. Chem. Phys.*, 1970, **53**, 1891.
14. Stewart, R. F., Davidson, E. R. and Simpson, W. T., *J. Chem. Phys.*, 1965, **42**, 3175.
15. Johnson, C. K., *ORTEP-II: A Fortran Thermal Ellipsoid Plot Program for Crystal Illustration*, ORNL-5138. Oak Ridge National Laboratory, Oak Ridge, Tennessee, (1976).
16. Tomizawa, H., Harada, K., Miki, E., Mizumachi, K., Ishimori, T., Urushiyama, A. and Nakahara, M., *Bull. Chem. Soc. Jpn*, 1993, **66**, 1658.
17. Haymore, B. L. and Ibers, J. A., *J. Am. Chem. Soc.*, 1975, **97**, 5369.
18. Elschenbroich, Ch. and Salzer, A., *Organotransition Metal Chemistry—A Concise Introduction*. VCH, Weinheim, Germany, 1989, p. 229.
19. Coll, R. K., Fergusson, J. K., McKee, V., Page, C. T., Robinson, W. T. and Keong, T. S., *Inorg. Chem.*, 1987, **26**, 106.